SUPPORTING INFORMATION

The first experimental charge density study using a Bruker AXS CMOS-type PHOTON 100 detector: the case of ammonium tetraoxalate dihydrate

Katarzyna N. Jarzembska,[a,b]* Radosław Kamiński,[b]
Łukasz Dobrzycki,[a]* Michał K. Cyrański[a]

[a] Department of Chemistry, University of Warsaw, Pasteura 1, 02-093 Warszawa, Poland

[b] Department of Chemistry, University at Buffalo, The State University of New York, Buffalo, NY 14260-3000, USA

1. R-factor definitions

Definitions of R-factors used in the *SORTAV* program include a number of counts for each reflection (y_{ik} – intensity value for the i-th reflection measured $k = 1 \ldots N_i$ times), and so are adjusted for small-sample measurement multiplicity.

(i) Relative mean absolute deviation of the measurements ('merging' R-factor, R_{mrg}[1]):

$$R_{\mathrm{mrg}} = \sum_i \sqrt{\frac{N_i}{N_i - 1}} \sum_k \left| y_{ik} - \langle y_i \rangle_k \right| \Big/ \sum_i \sum_k y_{ik}$$

(ii) Relative root-mean-square deviation of the measurements (RMS R-factor, R_{rms}):

$$R_{\mathrm{rms}} = \left[\sum_i \frac{N_i}{N_i - 1} \sum_k \left(y_{ik} - \langle y_i \rangle_k \right)^2 \Big/ \sum_i \sum_k y_{ik}^2 \right]^{1/2}$$

[1] This R-factor is sometimes called $R_{\mathrm{r.i.m.}}$ (see for example Rudolph, M. G., Wingren, C., Crowley, M. P., Chien, Y. & Wilson, I. A. (2004). *Acta Cryst.* **D60**, 656-664), or originally R_{meas} (Diederichs, K. & Karplus, P. A. (1997). *Nature Struct. Biol.* **4**, 269-275).

2. Additional figures

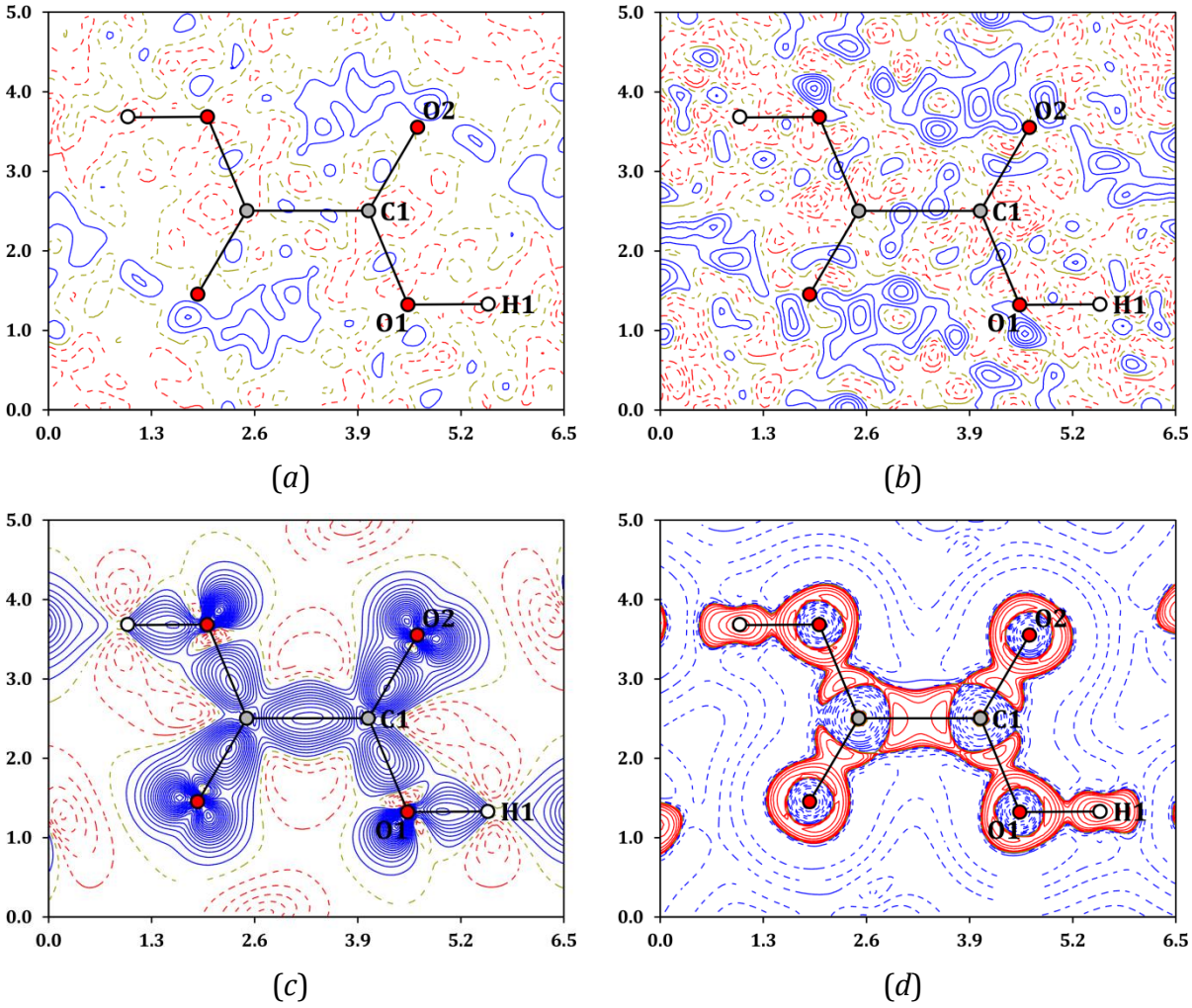

Figure 1S. (*a*,*b*) Residual density maps for the 1st oxalic acid molecule calculated either for reflections with $I \geq 3\sigma(I)$ (*a*), or for all reflections (*b*). (*c*,*d*) Deformation density (*c*) and negative Laplacian (*d*) maps for the same molecular fragment. (Contours and colour coding: (*a*,*b*,*c*) linear 0.05 e·Å^{-3} contours; blue solid lines – positive values, red dashed lines – negative values; (*d*) logarithmic contours; red solid lines – positive values, blue dashed lines – negative values.)

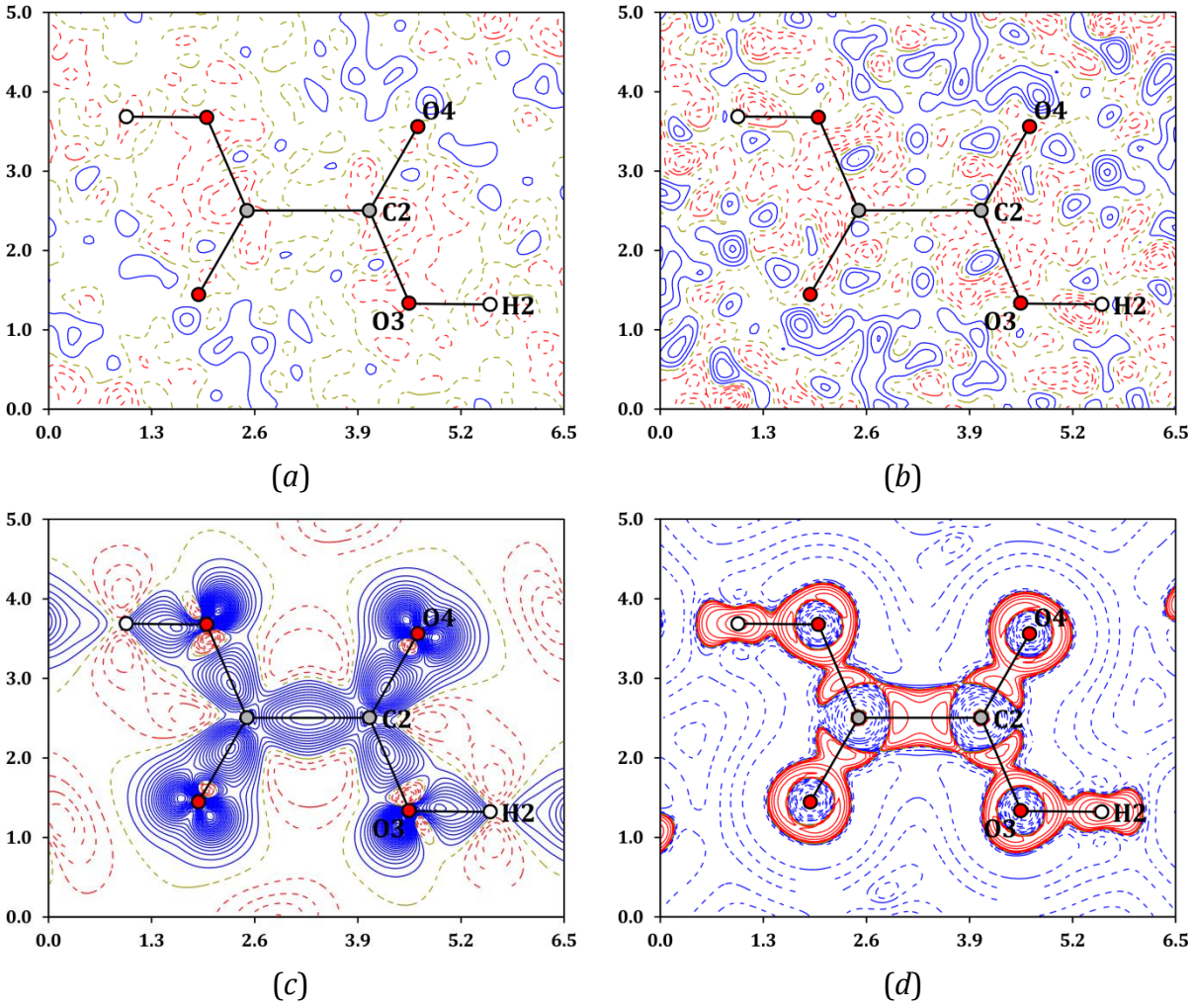

Figure 2S. (*a*,*b*) Residual density maps for the 2nd oxalic acid molecule calculated either for reflections with $I \geq 3\sigma(I)$ (*a*), or for all reflections (*b*). (*c*,*d*) Deformation density (*c*) and negative Laplacian (*d*) maps for the same molecular fragment. (Contours and colour coding: (*a*,*b*,*c*) linear 0.05 e·Å^{-3} contours; blue solid lines – positive values, red dashed lines – negative values; (*d*) logarithmic contours; red solid lines – positive values, blue dashed lines – negative values.)

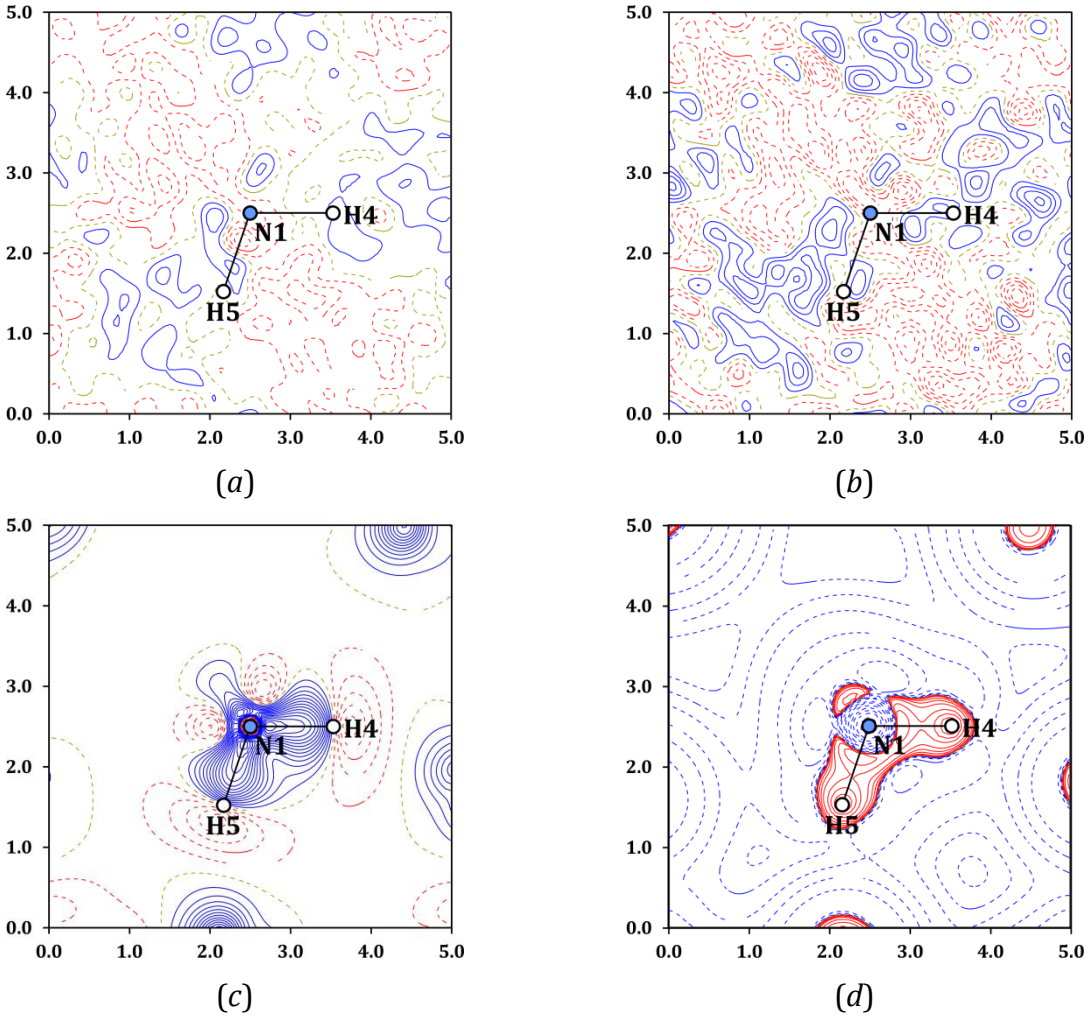

Figure 3S. (*a*,*b*) Residual density maps for the ammonium cation calculated either for reflections with $I \geq 3\sigma(I)$ (*a*), or for all reflections (*b*). (*c*,*d*) Deformation density (*c*) and negative Laplacian (*d*) maps for the same molecular fragment. (Contours and colour coding: (*a*,*b*,*c*) linear 0.05 e·Å^{-3} contours; blue solid lines – positive values, red dashed lines – negative values; (*d*) logarithmic contours; red solid lines – positive values, blue dashed lines – negative values.)

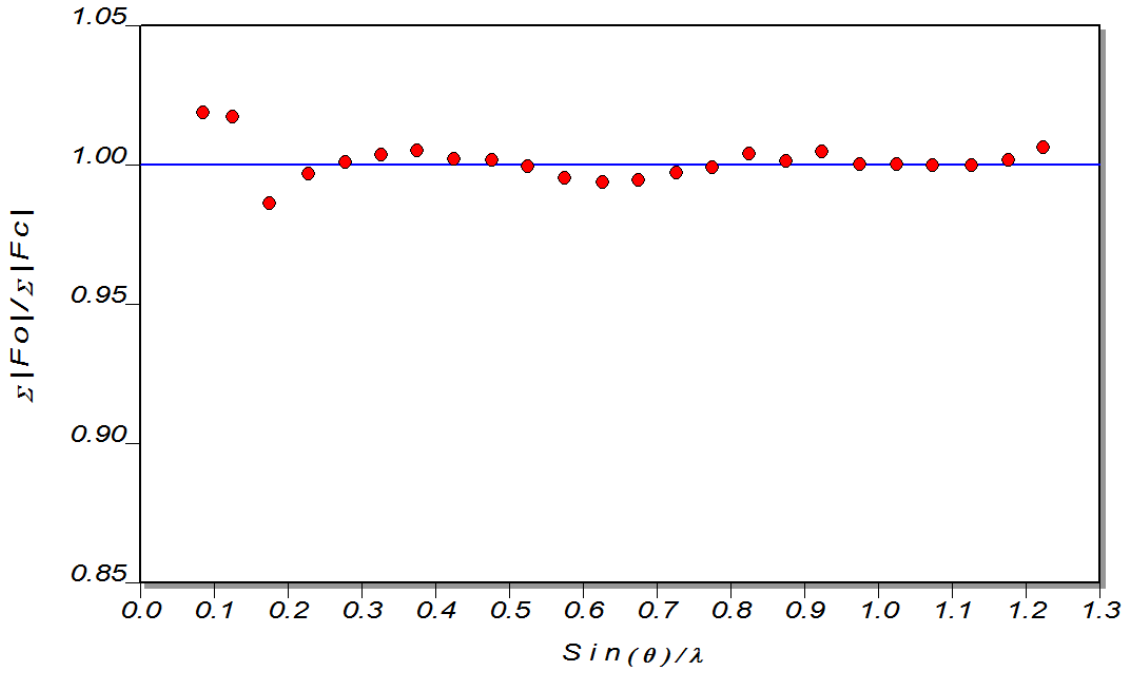

(*a*)

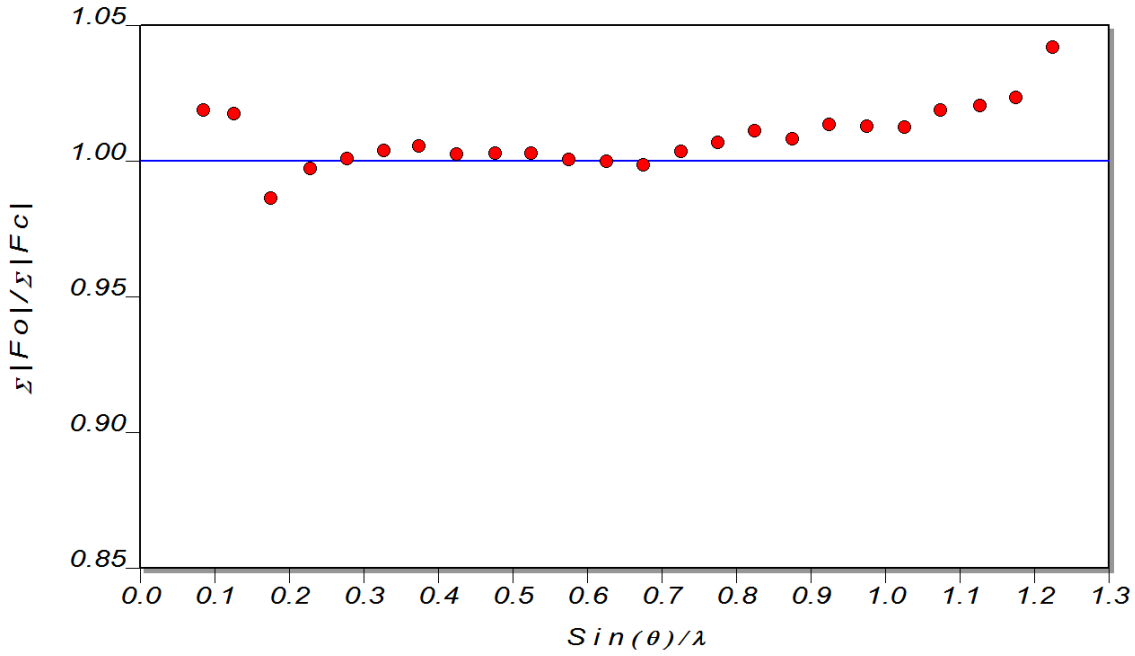

(*b*)

Figure 4S. Scale plot for the final refinement model (values of $\sin\theta/\lambda$ are given in $Å^{-1}$) calculated either for reflections with $I \geq 3\sigma(I)$ (*a*), or for all reflections (*b*).

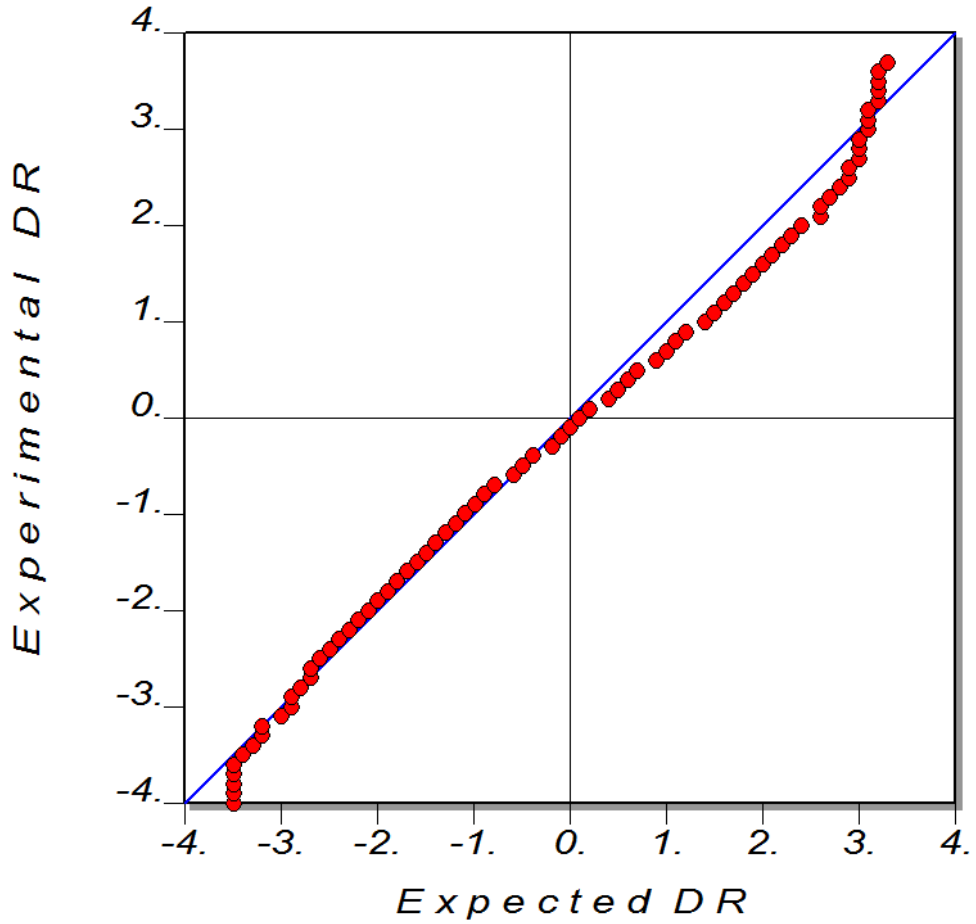

Figure 5S. Normal probability plot calculated for all reflections. The respective plot calculated for reflections with $I \geq 3\sigma(I)$ is practically identical.

3. Additional tables

Table 1S. Distribution of measured reflections in equal-volume resolution shells as taken from the *SORTAV* program after resolution cut-off ($s_{\max} = \sin\theta/\lambda_{\max}$ – maximal resolution for a given shell, N_{shell} – number of measured reflections in a given shell, N – average redundancy in a given shell, R_{mrg} and R_{rms} – R-factors corrected for small-sample measurement multiplicity, C – data completeness).

$s_{\max}$ / Å^{-1}	N_{shell}	N	$I/\sigma\ I$	R_{mrg}%	R_{rms}%	C%
0.46	750	6.1	35.20	2.50	6.83	99.9
0.58	755	4.7	24.58	2.24	2.20	100.0
0.66	741	3.1	18.98	3.65	3.82	99.5
0.73	732	2.6	16.96	3.26	2.78	99.2
0.79	757	3.3	16.63	3.93	3.54	99.5
0.84	725	3.8	15.95	4.55	4.00	99.5
0.88	741	4.8	18.27	4.18	3.62	99.1
0.92	770	4.3	15.26	5.13	4.39	98.6
0.96	723	4.4	15.77	5.05	4.10	98.6
0.99	735	3.9	12.80	6.34	5.35	99.1
1.02	741	3.1	11.99	6.06	4.90	97.8
1.05	707	2.1	9.37	6.81	5.34	96.5
1.08	751	2.9	9.39	8.24	6.50	96.3
1.11	545	2.1	8.44	7.47	5.37	76.5
1.14	649	2.4	8.01	8.39	6.29	85.4
1.16	693	2.6	7.79	9.52	7.61	91.3
1.18	670	2.6	7.31	10.02	7.63	91.4
1.21	677	2.8	7.97	9.23	7.07	90.4
1.23	699	2.7	7.12	10.31	8.20	92.3
1.25	665	2.4	6.00	12.15	9.66	89.4